

University of California - Davis

UCD-95-25

UCSD/PTH 95-16

October 1995

Detection of the Minimal Supersymmetric Model Higgs Boson H^0 in its $h^0 h^0 \rightarrow 4b$ and $A^0 A^0 \rightarrow 4b$ Decay Channels

J. Dai^a, J.F. Gunion^a, and R. Vega^c

^a*Physics Department, University of California, La Jolla, CA 92093, USA*

^b*Davis Institute for High Energy Physics, University of California, Davis, CA 95616, USA*

^c*Physics Department, Southern Methodist University, Dallas, TX 75275*

Abstract

We demonstrate that detection of the heavier minimal supersymmetric model CP-even Higgs boson H^0 will be possible at the LHC via its $H^0 \rightarrow h^0 h^0 \rightarrow 4b$ and/or $H^0 \rightarrow A^0 A^0 \rightarrow 4b$ decay channels for significant portions of the $(m_{A^0}, \tan\beta)$ model parameter space. At low m_{A^0} ($\lesssim 60$ GeV), *both* the $H^0 \rightarrow A^0 A^0 \rightarrow 4b$ and $H^0 \rightarrow h^0 h^0 \rightarrow 4b$ modes yield a viable signal for most $\tan\beta$ values; viability for the $h^0 h^0$ channel extends up to $m_{H^0} \sim 2m_t$ when the model parameter $\tan\beta$ is not large. At the Tevatron, the $h^0 h^0$ and $A^0 A^0$ channels are both potentially viable at low m_{A^0} for sufficiently good b -tagging efficiency and purity.

I. INTRODUCTION

The minimal supersymmetric standard model (MSSM) is currently the most attractive theory for physics below the TeV energy scale. The two Higgs doublets of the model (H_1 and H_2) are precisely the number required for: i) anomaly cancellations; ii) giving masses to both up quarks (H_2) and down quarks and leptons (H_1); and iii) nearly precise gauge coupling constant unification. While extra singlet Higgs fields can be added without affecting these crucial features, extra doublets or any number of Higgs triplet fields would destroy unification. Thus, it is vital to assess our ability to fully explore the Higgs sector of the MSSM at future colliders.

The physical Higgs bosons of the MSSM are: two CP-even Higgs boson, the h^0 and H^0 (with $m_{h^0} < m_{H^0}$ by definition); one CP-odd Higgs boson, the A^0 ; and a pair of charged Higgs bosons, H^\pm . The h^0 will very probably be detected at either LEP II or the LHC. However, the h^0 might well have properties very like those of the single Higgs boson h_{SM} of the minimal standard model (SM). The easiest, and perhaps only, way in which to verify that the Higgs sector is non-minimal would then be detection of a second Higgs boson. Unfortunately, our ability to do so at either the LHC or a future NLC is far from guaranteed. (The extensive literature on this subject is reviewed in Ref. [1].) Further, it would be highly desirable to be able to test the very explicit predictions for the self-couplings among the Higgs bosons of the MSSM. In this article, we demonstrate that, for the expected levels of b tagging efficiency and purity, the production/decay mode $gg \rightarrow H^0 \rightarrow h^0 h^0 \rightarrow b\bar{b}b\bar{b}$ will be observable at the LHC in important regions of the parameter space of the model, thereby allowing both detection of the H^0 and sensitivity to the $H^0 h^0 h^0$ coupling. We also show that when kinematically allowed the $H^0 \rightarrow A^0 A^0 \rightarrow 4b$ channel will be observable for most $\tan\beta$ values. In addition, we explore the observability of these modes at an upgraded Tevatron with integrated luminosity in the vicinity of $L = 30 \text{ fb}^{-1}$, and find statistically significant signals at small m_{A^0} , provided the efficiency and purity of b tagging are both excellent.

To begin, we note some key features of the MSSM Higgs sector. At tree-level, the Higgs sector is completely determined by the two parameters m_{A^0} and $\tan\beta = v_2/v_1$ (where v_1 and v_2 are the vacuum expectation values of the neutral components of the H_1 and H_2 doublets). After including

radiative corrections at one-loop [2] and two-loops [3,4], other parameters of the model, especially the top-quark (pole) mass m_t and the squark masses and mixings, have a strong influence on the Higgs sector. At large m_{A^0} ($\gtrsim 150$ GeV), m_{h^0} approaches an upper bound, while at small m_{A^0} , m_{H^0} approaches a lower bound, and both these bounds increase with increasing m_t and $m_{\tilde{t}}$. For m_{A^0} between 20 and 70-80 GeV, $m_{h^0} \sim m_{A^0}$ when $\tan \beta \gtrsim 4 - 6$.

For all the calculations of this paper we shall take $m_t = 175$ GeV, $m_{\tilde{t}} = 1$ TeV and neglect squark mixing. For these choices, one finds that m_{h^0} is sufficiently small, even after radiative corrections, that the $H^0 \rightarrow h^0 h^0$ decay channel is essentially always open for small to moderate $\tan \beta$, although strongly kinematically suppressed for m_{A^0} in the vicinity of ~ 90 GeV. For larger $\tan \beta$ values, the $H^0 \rightarrow h^0 h^0$ decay is allowed only for $m_{A^0} \lesssim 60$ GeV and $m_{A^0} \gtrsim 200$ GeV. For $m_{A^0} \lesssim 60$ GeV, the $H^0 \rightarrow A^0 A^0$ channel is also kinematically allowed. These kinematics, in combination with the complicated coupling patterns of the Higgs bosons, yield the $H^0 \rightarrow h^0 h^0$ branching ratio contours plotted in Fig. 1 in $(m_{A^0}, \tan \beta)$ parameter space. Full two-loop corrections to the H^0 and h^0 masses, mixing angles, and (very importantly) Higgs self-couplings have been included. We see that even though $H^0 \rightarrow h^0 h^0$ is generally kinematically allowed for $m_{A^0} \gtrsim 200$ GeV, $BR(H^0 \rightarrow h^0 h^0)$ is not guaranteed to be large; it is suppressed at large $\tan \beta$ values by the dominance of the enhanced $H^0 \rightarrow b\bar{b}, \tau^+ \tau^-$ modes and for $m_{H^0} \sim m_{A^0} \gtrsim 2m_t$ by the dominance of $t\bar{t}$ decays. In addition, we note that the $H^0 \rightarrow A^0 A^0$ mode generally has a sizeable branching ratio whenever it is kinematically allowed, *i.e.* for $m_{A^0} \lesssim 60$ GeV. Finally, the decays of the h^0 are essentially always dominated by $b\bar{b}$, as are those of the A^0 when m_{A^0} is small.

These results assume that SUSY decay channels are absent or negligible. When kinematically allowed, SUSY decays will be important for small to moderate $\tan \beta$ values and would suppress $BR(H^0 \rightarrow h^0 h^0)$.

II. LHC RESULTS

At the LHC, the channels that have been discussed for detection of the H^0 at moderate $\tan \beta$ and $m_{A^0} \lesssim 2m_t$ are $gg \rightarrow H^0$ production followed by (a) $H^0 \rightarrow ZZ^{(*)} \rightarrow 4\ell$, (b) $H^0 \rightarrow h^0 h^0 \rightarrow b\bar{b}b\bar{b}$

and (c) $H^0 \rightarrow h^0 h^0 \rightarrow b\bar{b}\gamma\gamma$, the inclusive $H^0 \rightarrow b\bar{b}$ channel having far too large a QCD background. The 4ℓ channel (a) has been the object of numerous theoretical and ATLAS+CMS experimental studies [5,1]. It has been shown to be viable for (roughly) $120 \text{ GeV} \lesssim m_{A^0} \lesssim 2m_t, \tan\beta \lesssim 1.5$ at low luminosity ($L = 30 \text{ fb}^{-1}$) and $70 \text{ GeV} \lesssim m_{A^0} \lesssim 2m_t, \tan\beta \lesssim 3 - 5$ at high luminosity ($L = 300 \text{ fb}^{-1}$). ATLAS and CMS have recently explored the $b\bar{b}\gamma\gamma$ mode (c). At $L = 300 \text{ fb}^{-1}$ it is viable when $BR(H^0 \rightarrow h^0 h^0) \gtrsim 0.05$ (see Fig. 1) and $m_{A^0} \gtrsim 120 \text{ GeV}$ [5,1]. The $b\bar{b}\gamma\gamma$ channel has small backgrounds, but the expected number of events is quite limited since the $h^0 \rightarrow \gamma\gamma$ branching ratio is of order 10^{-3} for much of parameter space. Here, we study whether the much higher rates in the $H^0 \rightarrow h^0 h^0 \rightarrow 4b$ channel can be utilized to detect the $H^0 \rightarrow h^0 h^0$ decays. In conjunction with the $2b2\gamma$ channel, this would also allow a model independent determination of the very important ratio $BR(h^0 \rightarrow \gamma\gamma)/BR(h^0 \rightarrow b\bar{b})$. In what follows, we demonstrate that the $4b$ channel will, indeed, allow detection of the H^0 in its $h^0 h^0$ decay mode in several important regions of parameter space, including a large region which overlaps that where the $2b2\gamma$ mode is viable. In addition, we find that, when kinematically allowed, the $H^0 \rightarrow A^0 A^0 \rightarrow 4b$ channel will be detectable.

We will consider three b -tagging scenarios. The first is what now seems to be a relatively conservative scenario taken from the SDC detector Technical Design Report [7] and employed in our earlier work [6]. As a function of p_T , $e_{b\text{-}tag}$ takes the values 0.16 at $p_T = 20 \text{ GeV}$, 0.22 at $p_T = 30 \text{ GeV}$, and is ≥ 0.3 for large p_T (yielding a rough average value of $e_{b\text{-}tag} \sim 0.25$); the probability of mis-tagging is taken to be $e_{mis\text{-}tag} = 0.01$ for all $p_T \geq 20 \text{ GeV}$. For this b -tagging scenario we assume a maximal yearly integrated luminosity of $L = 100 \text{ fb}^{-1}$. Current expectations further improve the situation. Canonical values now employed by ATLAS and CMS [5] are: $e_{b\text{-}tag} \sim 0.6$ and $e_{mis\text{-}tag} \sim 0.01$ for $|\eta| \leq 2.5$ and $p_T \geq 15 \text{ GeV}$ at low luminosity (applicable for accumulated luminosity of $L = 30 \text{ fb}^{-1}$); and $e_{b\text{-}tag} \sim 0.5$ and $e_{mis\text{-}tag} \sim 0.02$ for $|\eta| \leq 2.5$ and $p_T \geq 30 \text{ GeV}$ at high luminosity ($L = 300 \text{ fb}^{-1}$ accumulated). In the present work, we shall examine all three of these b -tagging scenarios; we shall label them (I), (II) and (III), respectively, in the order of the above discussion.

In this paper, we focus on $gg \rightarrow H^0$ production followed by $H^0 \rightarrow h^0 h^0 \rightarrow 4b$ or $H^0 \rightarrow A^0 A^0 \rightarrow$

$4b$ decay. The $gg \rightarrow b\bar{b}H^0$ cross section is not significantly enhanced in the regions of parameter space where $BR(H^0 \rightarrow h^0 h^0)$ is substantial (see Fig. 1), and, in fact, is small by comparison to the inclusive $gg \rightarrow H^0$ cross section in these regions. Although there is no special enhancement for the H^0 production rate, the $gg \rightarrow H^0 \rightarrow h^0 h^0 \rightarrow 4b$ ($gg \rightarrow H^0 \rightarrow A^0 A^0 \rightarrow 4b$) channels have the advantage over the previously-studied $gg \rightarrow b\bar{b}H^0 \rightarrow 4b$ channel that we can require two $2b$ combinations of mass $\sim m_{h^0}$ ($\sim m_{A^0}$) as well as a peak in the $4b$ mass. This considerably reduces both combinatoric and QCD backgrounds. Assuming 3 or 4 b -tagging, we find that the only possibly important backgrounds to the $H^0 \rightarrow h^0 h^0 \rightarrow 4b$ process are the irreducible $gg \rightarrow b\bar{b}b\bar{b}$ background and the mis-tag $gg \rightarrow b\bar{b}gg$ background (the intrinsic rate for this latter being very large). Because of the large size of m_t , the rate for $t\bar{t}b\bar{b}$ production is sufficiently smaller than that for $b\bar{b}b\bar{b}$ as to be neglectable, and the rate for $gg \rightarrow b\bar{b}q\bar{q}$ (summed over all light $q \neq b$) is much smaller than that for $gg \rightarrow b\bar{b}gg$. (We compute signal and background processes using exact parton level matrix elements.)

For the original conservative b -tagging scenario (I) it is difficult to maintain adequate event rates if we demand that 4 jets be tagged as b 's. Thus, in this case, we shall only require that 3 or 4 jets be tagged. The largest background is then from $b\bar{b}gg$ where at least one of the g 's is mis-tagged. For b -tagging scenarios (II) and (III) e_{b-tag} is sufficiently large that requiring 4 jets to be tagged as b 's leaves an adequate signal rate while suppressing the potentially large $gg \rightarrow b\bar{b}gg$ background to a level below the irreducible $gg \rightarrow b\bar{b}b\bar{b}$ background.

Semi-leptonic decays of the b -jets are included in our analysis. To incorporate detector resolution effects, we smear the lepton momenta using $\delta E/E = 0.2/\sqrt{E(GeV)} + 0.01$ and the quark momenta using $\delta E/E = 0.5/\sqrt{E(GeV)} + 0.03$. If a b -jet decays semi-leptonically, we replace the jet momentum by the sum of the (smeared) lepton and light quark momenta; otherwise, we employ the full (smeared) b -jet momentum. Approximate techniques for compensating for the momentum lost to the neutrino in the case of a semi-leptonic decay have not been employed here; implementation of such a technique might improve our results.

The precise cuts imposed are adjusted according to the (presumed) masses of the H^0 and h^0 (or

A^0). In the following we use the generic notation h for the h^0 or light A^0 . First, we required that there be two jet pairs each having pair mass in the interval $[0.88m_h, 1.08m_h]$. Second, we required that the $4b$ mass be in an appropriate interval: $[115, 135]$, $[140, 160]$, $[160, 185]$, $[180, 210]$, $[235, 260]$, $[285, 310]$, $[330, 360]$, $[380, 415]$, $[430, 465]$, and $[475, 515]$ for $m_{H^0} = 125, 150, 175, 200, 250, 300, 350, 400, 450$, and 500 , respectively (all masses in GeV). These mass intervals in m_h and m_{H^0} are roughly optimal for the smearing outlined above. They extend further below the nominal mass than above so as to capture more of the low mass tail resulting from semi-leptonic b decays.

We will also impose a cut requiring that the transverse missing energy be less than 35 GeV. This cut does not significantly reduce the signal rate since signal events with substantial missing energy will not pass the m_h cuts anyway. This is because there are typically several semi-leptonic b decays in events with large \cancel{E}_T , making it quite likely that one or more of the pairs of b quarks that come from the decay of the h 's will not reconstruct to a pair mass close to m_h . In contrast, the $\cancel{E}_T \leq 35$ GeV cut removes the substantial percentage of background events where the semi-leptonic b decays lead to large missing energy. We note that in computing the missing energy and determining the optimal cut, we have included an estimate of the missing energy associated with the underlying minimum-bias event structure.

For each choice of m_{H^0} and m_h we considered two possible p_T^{\min} cut options and two possible cuts on the minimum separation required between any two of the b jets, ΔR^{\min} . These were $p_T^{\min} = 15$ or 30 GeV and $\Delta R^{\min} = 0.7$ or 1.2. (Note that the $p_T^{\min} = 15$ GeV cut cannot be employed in the high luminosity scenario III, and that for scenario I the effective minimum is 20 GeV.) For any given combination of m_{H^0} , m_h masses the choice among these four $(\Delta R^{\min}, p_T^{\min})$ options which gives the largest significance for the signal is chosen. Generally speaking, it is advantageous to impose the strongest cuts that one can without harming the efficiency of acceptance too severely. Roughly, for lower values of $m_{H^0} \lesssim 200$ GeV, the lower p_T^{\min} must be employed, whereas for $m_{H^0} \gtrsim 200$ GeV the higher p_T^{\min} was generally more optimal. When m_{H^0} is large and m_h is small, the h boost in the H^0 center of mass is often such that the smaller ΔR^{\min} must be employed.

Our procedure was to tabulate the signal and background rates for a series of m_{H^0} masses and

m_h masses that scanned all m_{H^0} values of possible interest and all m_h values for which $H^0 \rightarrow hh$ is allowed by kinematics, for each of the four $(\Delta R^{\min}, p_T^{\min})$ options described above. (Of course, only the two ΔR^{\min} options were examined in the high-luminosity b -tagging case (III) for which $p_T^{\min} = 30$ GeV is required.) Rates corresponding to the best of these options for each m_{H^0}, m_h (in terms of statistical significance) were then entered into a final summary table. SUSY relations between m_{H^0} and m_h were not implemented in constructing the tables. Signal event rates for $gg \rightarrow H^0 \rightarrow hh \rightarrow 4b$ were obtained assuming 100% branching ratio for the decays $H^0 \rightarrow hh$ and $h \rightarrow b\bar{b}$ and assuming a width $\Gamma(H^0 \rightarrow gg) = 5 \times 10^{-4}$ GeV, that is typical of the values obtained in the MSSM. In order to determine the actual statistical significance of the $gg \rightarrow H^0 \rightarrow h^0 h^0 \rightarrow 4b$ and $gg \rightarrow H^0 \rightarrow A^0 A^0 \rightarrow 4b$ signals as a function of location in the MSSM parameter space, rates were obtained for the appropriate m_{H^0} and $m_h = m_{h^0}$ (or $m_h = m_{A^0}$) values by interpolation between entries in the summary table, and the branching ratios and gg width were adjusted according to the predicted MSSM values. In our considerations, m_h masses below 20 GeV are not considered nor are m_{H^0} masses below 110 GeV. The contours presented below correspond to setting statistical significances to zero for such cases.

It is not appropriate here to detail the signal and background rates tabulated in the summary table. We confine ourselves to a few comments.

1. b -tagging option (I): 3 or 4 b -tags, $L = 100 \text{ fb}^{-1}$ — In this case, after cuts and tagging the $gg \rightarrow H^0 \rightarrow 4b$ signal and $gg \rightarrow 4b$ background rates are typically comparable, whereas the $gg \rightarrow 2b2g$ mis-tag background rate is a factor of 3-9 higher.
2. b -tagging option (II): low luminosity ($L = 30 \text{ fb}^{-1}$), 4 b -tags — Here, the $gg \rightarrow H^0 \rightarrow 4b$ rate is somewhat larger than the $gg \rightarrow 4b$ irreducible background rate, which, in turn, is a factor of at least 10 larger than the $bb \rightarrow 2b2g$ rate — *i.e.* the latter background becomes unimportant when $4b$'s are tagged with excellent efficiency and purity.
3. b -tagging option (III): high luminosity ($L = 300 \text{ fb}^{-1}$), 4 b -tags — The $p_T^{\min} = 30$ GeV rates are obtained from those in option (II) by multiplying the rates for $4b$ final state channels

by the factor $(0.5/0.6)^4 \times 10 \simeq 4.8$ and the rates for the $2b2g$ background by $(0.5/0.6)^2 \times (0.02/0.01)^2 \times 10 \simeq 27.8$. In this case, the $2b2g$ background rates are typically comparable to the $4b$ background rates.

The relation between the option (I) and option (II) rates is easily understood. Very roughly, the signal and $gg \rightarrow 4b$ rates for option (I) are

$$\propto \left\{ 4 \times (e_{b\text{-tag}} \sim 0.25)^3 \times [(1 - e_{b\text{-tag}}) \sim 0.75] + (e_{b\text{-tag}} \sim 0.25)^4 \right\} \times 100 \text{ fb}^{-1} = 5.1 \text{ fb}^{-1}$$

(the factor of 4 corresponding to any one of the 4 b 's remaining untagged), while those for option (II) are $\propto (e_{b\text{-tag}} = 0.6)^4 \times 30 \text{ fb}^{-1} = 3.9 \text{ fb}^{-1}$. In contrast, in going from option (I) to option (II) the $gg \rightarrow 2b2g$ rates are suppressed by a factor of roughly

$$\frac{(0.6)^2 \times (0.01)^2 \times 30 \text{ fb}^{-1}}{(0.25)^2 \times 0.01 \times 2 \times 100 \text{ fb}^{-1}} \sim 0.0086$$

where the extra factor of 2 in the denominator corresponds to allowing either of the g 's to not be (mis-)tagged in the 3 b -tag case. The result is that the $4b$ rates for option (II) are comparable to those for option (I), and that in option (II) the $b\bar{b}gg$ background is substantially smaller than the $b\bar{b}b\bar{b}$ irreducible background. In option (III) the $4b$ and $2b2g$ backgrounds become comparable due to the lower efficiency for b tagging, coupled with a higher rate for mis-tagging. Clearly, b -tagging expectations (II) and (III) yield better statistical significance for the signal than the conservative choices of (I), for the same integrated luminosity.

Finally, we recall that at high luminosity it is assumed that 30 GeV is the lowest p_T^{\min} value that can be employed. This effectively restricts the high luminosity option (III) case to m_{H^0} values above about 150 GeV.

In order to compute the statistical significance of a signal when both the $H^0 \rightarrow A^0 A^0$ and $H^0 \rightarrow h^0 h^0$ decays are present (low m_{A^0}) we must take into account the fact that $m_{h^0} \sim m_{A^0}$ at low m_{A^0} once $\tan \beta \gtrsim 4-6$. Our procedure is to include in the $h^0 h^0$ ($A^0 A^0$) signal event rate the portion of the $A^0 A^0$ ($h^0 h^0$) signal event rate that overlaps into the double $[0.88m_{h^0}, 1.08m_{h^0}]$ ($[0.88m_{A^0}, 1.08m_{A^0}]$) pair mass window. Obviously, when m_{A^0} and m_{h^0} are very close, this simply means the signal rates

are added together before the statistical significance $N_{SD} = S/\sqrt{B}$ is computed. Our procedure implies that the contours for the $h^0 h^0$ and $A^0 A^0$ modes will converge for $\tan \beta \gtrsim 4 - 6$.

We display in Fig. 2 the $N_{SD} = 2, 5$, and 10 discovery contours for $H^0 \rightarrow h^0 h^0$ and $H^0 \rightarrow A^0 A^0$ for the $L = 30 \text{ fb}^{-1}$ and $L = 300 \text{ fb}^{-1}$ b -tagging options (II) (window 1) and (III) (window 2). It turns out that the results for b -tagging option (I) for $L = 100 \text{ fb}^{-1}$ are almost identical to those for option (II) at $L = 30 \text{ fb}^{-1}$ and so we do not present them here.

In the $L = 30 \text{ fb}^{-1}$ option (II) case, we see two distinct regions. At low m_{A^0} values there is a narrow band in the $20 \text{ GeV} \lesssim m_{A^0} \lesssim 60 \text{ GeV}$ region for which $N_{SD} \geq 5$ in both the $h^0 h^0$ and $A^0 A^0$ modes. (The $h^0 h^0$ mode is viable for slightly more parameter space as indicated by its contours which bulge a bit beyond those for the $A^0 A^0$ mode at lower $\tan \beta \lesssim 6$ values.) The lower m_{A^0} limits of these contours are an artifact of our zeroing all rates when the light Higgs mass is below 20 GeV — in any case, we already know from LEP I that $m_{A^0} \geq 40 \text{ GeV}$. At higher m_{A^0} values there is a $N_{SD} \geq 5$ region for the $h^0 h^0$ mode, extending from roughly $m_{A^0} \sim 100 \text{ GeV}$ up to $m_{A^0} \gtrsim 2m_t$ for $\tan \beta \lesssim 4$. Note that a viable signal is maintained for m_{H^0} somewhat beyond $2m_t$, despite the fact that $H^0 \rightarrow t\bar{t}$ decays rapidly become dominant. This is because the top-quark loop contribution to the $gg \rightarrow H^0$ coupling is substantially enhanced in the vicinity of $m_{H^0} \sim 2m_t$, thereby enhancing the $gg \rightarrow H^0$ production rate.

In the $L = 300 \text{ fb}^{-1}$ option (III) case, the bands at low m_{A^0} disappear; the $p_T > 30 \text{ GeV}$ cut eliminates them by virtue of kinematics. The $N_{SD} \geq 5$ region for $H^0 \rightarrow h^0 h^0 \rightarrow 4b$ at large m_{A^0} extends to $\tan \beta \lesssim 5$ and slightly higher m_{A^0} values.

III. TEVATRON RESULTS

In this section, we explore the capability of the Tevatron to observe the $H^0 \rightarrow h^0 h^0$ and $H^0 \rightarrow A^0 A^0$ signals in the $4b$ final state. CDF and D0 have dramatically increased their b -tagging efficiency and purity. At an upgraded Tevatron, they now expect to achieve $e_{b\text{-tag}} \sim 0.5$ with $e_{\text{mis-tag}} \sim 0.005$ for a b -jet with $p_T \gtrsim 15 \text{ GeV}$ and $|\eta| < 2$ at instantaneous luminosities capable of yielding $L = 10 - 30 \text{ fb}^{-1}$ per year [8]. Their ability to obtain such a very small mis-tagging probability is crucial

at the Tevatron, since the low event rates make it necessary to accept events in which either 3 or 4 b 's are tagged.

Our results for $L = 30 \text{ fb}^{-1}$ are displayed in Fig. 3. For the above-stated b -tagging efficiency and purity (left window of figure), a $N_{SD} = 4$ ($N_{SD} = 2$) signal is obtained for $33 \lesssim m_{A^0} \lesssim 53 \text{ GeV}$ ($25 \lesssim m_{A^0} \lesssim 55 \text{ GeV}$) in both the $h^0 h^0$ and $A^0 A^0$ modes (with the $h^0 h^0$ mode contours again bulging a bit beyond the $A^0 A^0$ contours for $\tan \beta \lesssim 6$). If the detector design can be further improved, so as to achieve $e_{b\text{-tag}} \sim 0.75$ and $e_{mis\text{-tag}} \sim 0.0025$, the $h^0 h^0$ and $A^0 A^0$ signals will be promoted to at least the $N_{SD} = 5$ level (inner contours of the right-hand window) for most of this low m_{A^0} band. The region for which $H^0 \rightarrow h^0 h^0$ is observable at higher m_{A^0} is much more restricted than at the LHC.

We note that the near degeneracy of the A^0 and h^0 in the low- m_{A^0} region is quite critical to there being an observable level for the H^0 signal at the Tevatron. After cuts, tagging, and mass binning, the $4b$ background is typically of order fifty to two hundred events and the $2b2g$ background ranges from several hundred to more than a thousand events. The $A^0 A^0$ and $h^0 h^0$ signals, if not simultaneously present, would typically be just below the observable level; but in combination, they provide a just adequate event rate.

IV. DISCUSSION AND CONCLUSIONS

We have demonstrated that detection of $gg \rightarrow H^0 \rightarrow h^0 h^0$ in $4b$ final states at the LHC will be possible for a substantial portion of parameter space, for anticipated integrated luminosities and b -tagging efficiency and purity. Should m_{A^0} turn out to be small ($\lesssim 60 \text{ GeV}$), then *both* $H^0 \rightarrow h^0 h^0 \rightarrow 4b$ and $H^0 \rightarrow A^0 A^0 \rightarrow 4b$ yield viable signals. These channels add to the growing list of signals that can provide probes of the MSSM Higgs sector at the LHC [1]. Detection of the H^0 in the $h^0 h^0$ and $A^0 A^0$ modes at the Tevatron is mostly limited to the $m_{A^0} \lesssim 55 \text{ GeV}$ portion of parameter space, and requires accumulated luminosity of $L \sim 30 \text{ fb}^{-1}$ as well as excellent b -tagging efficiency and purity.

Although observation of $e^+ e^- \rightarrow h^0 A^0$ production at LEP II would also be possible in the low

m_{A^0} region of parameter space, the information gained about the Higgs sector from detection at the Tevatron (or LHC) of $gg \rightarrow H^0 \rightarrow h^0 h^0, A^0 A^0$ would be very complementary.

In our analysis, we have assumed that it will be possible to trigger on the $4b$ final states, perhaps by requiring 4 jets with $p_T > 15$ to 20 GeV, or via a fast b -vertex trigger, or some combination of these approaches. This issue is under study by the ATLAS and CMS collaborations.

We note that our computations have not included higher-order QCD K factors for either signal or backgrounds. The K factor for $gg \rightarrow H^0$ is known to be substantial ($K \sim 1.6$ [9]) and presumably those for the backgrounds will also be significant. Assuming that all K factors are of similar size (if anything the $gg \rightarrow H^0$ K factor is likely to be the largest), the quoted statistical significances for observation will be increased by a factor of \sqrt{K} .

The rate for $gg \rightarrow H^0 \rightarrow h^0 h^0, A^0 A^0$ probes the product, $\Gamma(H^0 \rightarrow gg) \times BR(H^0 \rightarrow h^0 h^0, A^0 A^0)$, which is sensitive to the $H^0 \rightarrow gg$ one-loop coupling and the tri-linear Higgs self couplings. $\Gamma(H^0 \rightarrow gg)$ can deviate significantly from the values employed here if squarks are light, or if there are other unobserved heavy colored particles with significant couplings to the H^0 . The tri-linear Higgs couplings could also deviate from MSSM predictions if, for example, Higgs singlet fields are added to the minimal two-doublet structure. In the very substantial portion of parameter space where both $H^0 \rightarrow h^0 h^0 \rightarrow 4b$ and $H^0 \rightarrow h^0 h^0 \rightarrow 2b2\gamma$ can be observed at the LHC, the ratio of the $h^0 \rightarrow \gamma\gamma$ and $h^0 \rightarrow b\bar{b}$ couplings can be extracted. Clearly, much important information regarding the SUSY Higgs sector, and many important checks of the MSSM, will be made possible by observation of the $H^0 \rightarrow h^0 h^0$ and/or $A^0 A^0$ modes.

In Ref. [6], we demonstrated that detection of $gg \rightarrow b\bar{b}H^0$ and/or $gg \rightarrow b\bar{b}A^0$ in $4b$ final states is possible for sufficiently large $\tan\beta$ values (the required $\tan\beta$ value increases as m_{A^0} increases). Updated results that incorporate the current more optimistic expectations for b -tagging efficiency and purity will appear shortly [10]. The region of the $(m_{A^0}, \tan\beta)$ parameter space for which the above modes are observable is largely complementary to that for which we have demonstrated viability for the $4b$ final states resulting from $gg \rightarrow H^0 \rightarrow h^0 h^0$ and/or $gg \rightarrow H^0 \rightarrow A^0 A^0$. In combination, these two different types of $4b$ modes allow H^0 and/or A^0 detection over a very

sizeable fraction of the $(m_{A^0}, \tan \beta)$ parameter space plane when $m_{A^0} \lesssim 400$ GeV. There is a wedge between the discovery regions at moderate $\tan \beta \gtrsim 5$ that grows as m_{A^0} increases above 400 GeV. Further improvements in b -tagging efficiency and purity would substantially reduce this wedge. Efforts by the ATLAS and CMS collaborations in this direction are thus highly desirable. Overall, the $4b$ modes have considerably enhanced the prospects for detecting the H^0 and/or the A^0 at the LHC. It is thus quite possible that the LHC will be able to fully explore the Higgs sector of the MSSM.

ACKNOWLEDGMENTS

This work was supported in part by the U.S. Department of Energy. Further support was provided by the Davis Institute for High Energy Physics.

REFERENCES

1. An extensive review of the subject appears in J.F. Gunion, A. Stange, and S. Willenbrock, ‘Weakly-Coupled Higgs Bosons’, to appear in *Electroweak Symmetry Breaking and Beyond the Standard Model*, ed. T. Barklow, S. Dawson, H. Haber, and J. Siegrist, World Scientific Publishing.
2. For a review, see H. Haber, in *Perspectives on Higgs Physics*, ed. G. Kane, World Scientific Publishing, p. 79.
3. M. Carena, J.R. Espinosa, M. Quiros and C.E.M. Wagner, CERN-TH/95-45; J.A. Casas, J.R. Espinosa, M. Quiros and A. Riotto, Nucl. Phys. **B436**, 3 (1995).
4. H. Haber, R. Hempfling and A. Hoang, CERN-TH/95-216.
5. F. Gianotti (ATLAS), presented at the European Physical Society International Europhysics Conference on High Energy Physics, Brussels, Belgium, July 27 - August 2, 1995, and private communication. R. Kinnunen (CMS), presentation at the Tahoe CMS Week, Tahoe City, CA,

September 25-27, 1995.

6. J. Dai, J. Gunion, and R. Vega, Phys. Lett. **B345**, 29 (1995).
7. Technical Design Report, SDC Collaboration.
8. S. Kuhlmann, CDF note CDF/PHYS/ELECTROWEAK/PUBLIC/3342, September, 1995.
J. Womersley, private communication.
9. For a review and references, see B. Kniehl, Int. J. Mod. Phys. **A10**, 443 (1995.)
10. J. Dai, J.F. Gunion, and R. Vega, in preparation.

FIGURES

1. We show contours of fixed $BR(H^0 \rightarrow h^0 h^0) = 0.5, 0.2, 0.1$ and 0.05 in the $(m_{A^0}, \tan \beta)$ parameter space. We have taken $m_t = 175$ GeV (pole mass) and $m_{\tilde{\tau}} = 1$ TeV, and neglected squark mixing. The $0.2, 0.1$ and 0.05 contours in the vicinity of $m_{A^0} \sim 60$ GeV are essentially indistinguishable; the $H^0 \rightarrow h^0 h^0$ decay becomes kinematically disallowed for m_{A^0} values just beyond this boundary.
2. We show the $(m_{A^0}, \tan \beta)$ parameter space contours within which $H^0 \rightarrow h^0 h^0 \rightarrow 4b$ and $H^0 \rightarrow A^0 A^0 \rightarrow 4b$ can be observed at the $2, 5$, or 10σ level assuming: 1) an integrated luminosity of $L = 30 \text{ fb}^{-1}$ and 4- b -tagging option (II); and 2) $L = 300 \text{ fb}^{-1}$ and 4- b -tagging option (III). See text for details. We take $m_t = 175$ GeV and include two-loop radiative corrections, assuming $m_{\tilde{\tau}} = 1$ TeV and neglecting squark mixing. We also assume that SUSY decays are absent.
3. We show the $(m_{A^0}, \tan \beta)$ parameter space contours within which $H^0 \rightarrow h^0 h^0, A^0 A^0 \rightarrow 4b$ can be observed: 1) at the $2, 4 \sigma$ level assuming $e_{b\text{-}tag} = 0.5$ and $e_{mis\text{-}tag} = 0.005$; and 2) at the $3, 5 \sigma$ level assuming $e_{b\text{-}tag} = 0.75$ and $e_{mis\text{-}tag} = 0.0025$. We assume $\sqrt{s} = 1.8$ TeV, an integrated luminosity of $L = 30 \text{ fb}^{-1}$ and accept events in which either 3 or 4 b 's with $p_T > 15$ GeV and $|\eta| < 2$ are tagged.

FIGURES

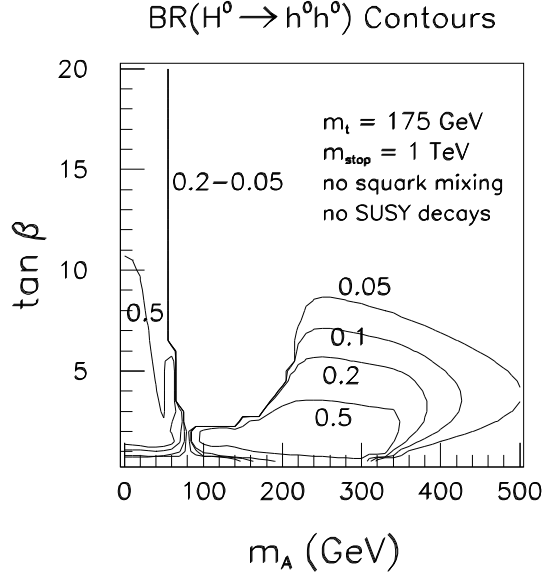


FIG. 1. We show contours of fixed $BR(H^0 \rightarrow h^0 h^0) = 0.5, 0.2, 0.1$ and 0.05 in the $(m_{A^0}, \tan \beta)$ parameter space. We have taken $m_t = 175$ GeV (pole mass) and $m_{\tilde{t}} = 1$ TeV, and neglected squark mixing. The $0.2, 0.1$ and 0.05 contours in the vicinity of $m_{A^0} \sim 60$ GeV are essentially indistinguishable; the $H^0 \rightarrow h^0 h^0$ decay becomes kinematically disallowed for m_{A^0} values just beyond this boundary.

LHC $H^0 \rightarrow h^0 h^0, A^0 A^0$ Detection

4 b tagging, $|\eta^b| < 2.5$

$N_{SD}=2, 5, 10$ Contours

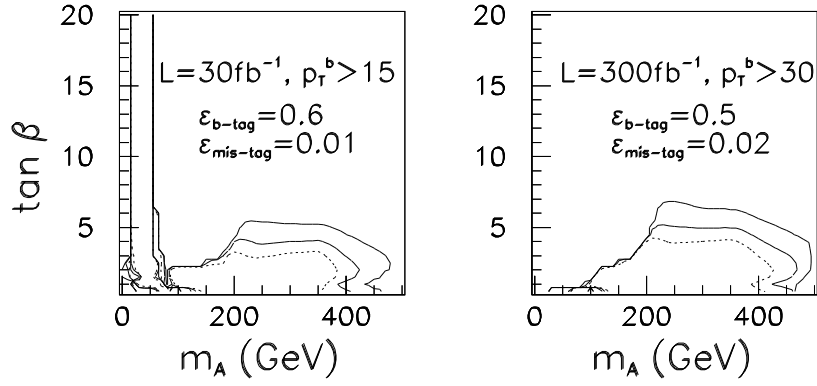


FIG. 2. We show the $(m_{A^0}, \tan \beta)$ parameter space contours within which $H^0 \rightarrow h^0 h^0, A^0 A^0 \rightarrow 4b$ can be observed at the 2, 5, or 10σ level assuming: 1) an integrated luminosity of $L = 30 \text{ fb}^{-1}$ and 4- b -tagging option (II); and 2) $L = 300 \text{ fb}^{-1}$ and 4- b -tagging option (III). See text for details.

Tevatron $H^0 \rightarrow h^0 h^0, A^0 A^0$ Detection
 3 b tagging, $p_T^b > 15$ GeV, $|\eta^b| < 2$
 $L = 30 \text{ fb}^{-1}$

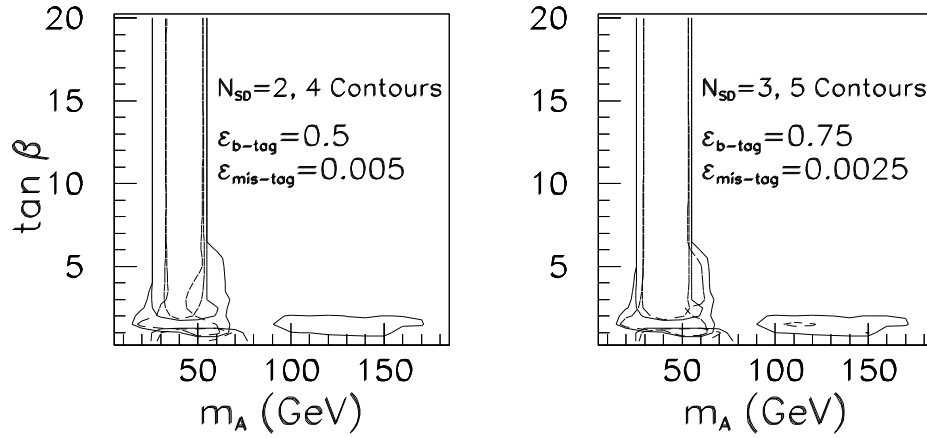


FIG. 3. We show the $(m_{A^0}, \tan \beta)$ parameter space contours within which $H^0 \rightarrow h^0 h^0, A^0 A^0 \rightarrow 4b$ can be observed: 1) at the 2, 4 σ level assuming $\epsilon_{b\text{-tag}} = 0.5$ and $\epsilon_{mis\text{-tag}} = 0.005$; and 2) at the 3, 5 σ level assuming $\epsilon_{b\text{-tag}} = 0.75$ and $\epsilon_{mis\text{-tag}} = 0.0025$. We assume $\sqrt{s} = 1.8$ TeV, an integrated luminosity of $L = 30 \text{ fb}^{-1}$ and accept events in which either 3 or 4 b 's with $p_T > 15$ GeV and $|\eta| < 2$ are tagged.